Range-Doppler Tracking of Ships using Single-Channel Airborne Radar Data

Sushil Kumar Joshi, Stefan V. Baumgartner
Microwaves and Radar Institute, German Aerospace Center (DLR), Oberpfaffenhofen, Germany

Abstract

Ship tracking is important to ensure maritime safety and security. However, with the state-of-the-art sensors and systems detecting several maritime threats is still a very challenging task. In this paper, a supportive ship tracking concept using range-compressed (RC) airborne radar data is proposed. Ships are tracked in the range-Doppler domain where the ships moving with certain line-of-sight velocity appear out of the clutter region, thus improving their detectability. Ship tracking in high resolution data is an extended target tracking problem, therefore the extracted centroids of the detected and clustered ships are tracked over time. A powerful track management system is also developed for recognizing and terminating the false targets. Simulated and real experimental results from the DLR's F-SAR and DBFSAR system are provided to prove the concept.

1. Introduction

Frequent ship monitoring is crucial for the maritime situational awareness. Current operational surveillance systems used for the monitoring purposes are the AIS (automatic identification system) and the marine radars. Airborne radar sensor can give additional support to these systems by detecting ships that are not equipped with the AIS transponders and also undetectable from marine radars.

Airborne radars while flying along the azimuth direction transmit its pulse in the range direction. They are capable of collecting the data with very high resolution and with shorter revisit and long observation times. The performance of these radar platforms is often limited by the aircraft's endurance which in future can be overcome by installing them on high-altitude platforms (HAP) or high-altitude pseudo satellites (HAPS) which are flying in the stratosphere for several days, weeks, months or even years [1].

We use range-compressed (RC) data for the airborne radar-based maritime surveillance. When airborne radars or future HAP or HAPS are used, the signal-to-noise ratio is sufficiently large, therefore there is not a need to use fully focused radar images. This saves the additional signal processing efforts and enable the development of real-time capable systems [2].

Ships are detected in the range-Doppler domain after applying the azimuth fast Fourier transform to the RC data. The primary advantage of detecting ships in Doppler domain is that if ships even of low radar cross section move with sufficient line-of-sight velocity, they are shifted out of clutter region, thus improving their detection capability (cf. **Figure 1(b)**).

Like detection, ships are also tracked in range-Doppler domain. Tracking in range-Doppler has a benefit that overlapping target signals in time domain are most likely to be separated in range-Doppler domain. This is advantageous for tracking multiple targets in a dense multi-target scenario. Target tracks are needed (1) for generating high resolution inverse synthetic aperture radar (ISAR) images by successively extracting the ship data and also, (2) for fusing with the simultaneously acquired AIS data by mapping the detections on ground after computing additionally the direction-of-arrival (DOA) angle of the target. Therefore, tracking in is a pre-requisite for the aforementioned applications.

In the paper, a concept of range-Doppler based ship tracking using RC airborne radar data is proposed. Extended targets in high-resolution data give more than one detection per target. Therefore, we extract the ship centroid and track them in range-Doppler using a suitable target motion model. The overall multi-target tracking system is designed using a database structure. Other associated challenges while tracking in range-Doppler like data association in case of multi-target tracking, missed and false detections are also discussed. Simulated and real experimental data from DLR's (German Aerospace Center) airborne F-SAR [3] and DBFSAR [4] system are used to validate the proposed method.

2. Detection and clustering

Ships are detected in range-Doppler domain using the methodology proposed in [2]. In that paper the authors have proposed a detection algorithm suitable for detecting targets in range-Doppler domain. After obtaining multiple pixel-based detections of the ship in the data, a standard DBSCAN (density based spatial clustering of applications with noise) algorithm [5] is used to form the ship cluster. An example of a real ship cluster in real X-band HH polarized F-SAR data is shown in **Figure 1**.

For tracking, the center of the clustered ship, i.e., its Doppler frequency and range positions (cf. **Figure 1(b)**) are tracked at successive times. In our case the cluster center is the center of gravity (COG) of the cluster. Compared to other estimation methods like center corresponding to the maximum peak amplitude or the center of the bounding box, we found COG to be more stable for most of the investigated ships in the experimental airborne radar data [6].

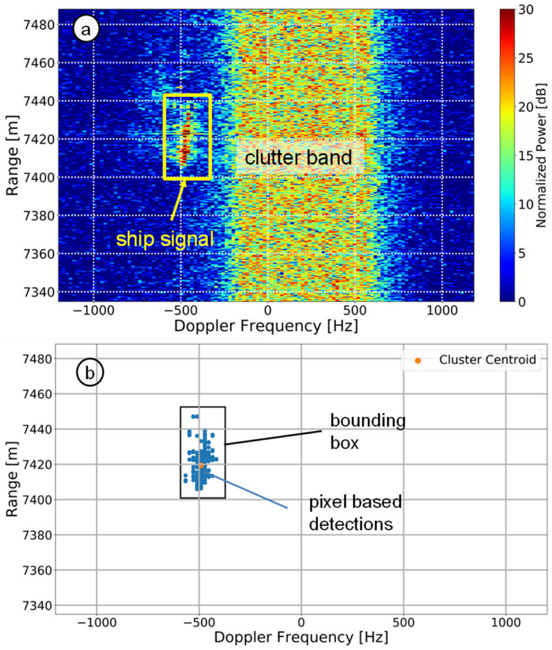

Figure 1 (a) Real X-band HH polarized RC airborne radar data in range-Doppler domain at a specific azimuth time. A ship (in exo-clutter region) and the clutter band are shown in the figure. (b) Clustered pixel-based detections belonging to the ship with its bounding box.

3. Tracking in range-Doppler

Figure 2 shows a schematic representation of the range-Doppler based tracking concept using RC data.

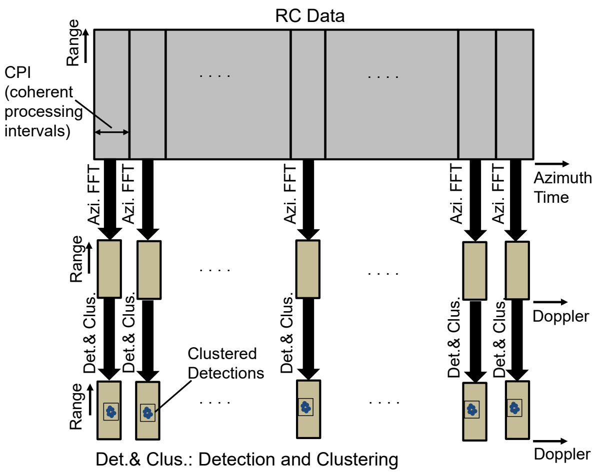

Figure 2 Illustration of the series of range-Doppler data used for target tracking. Detected and clustered ship at each CPI are shown in the figure.

As shown in the **Figure 2**, the RC data is first partitioned along azimuth into smaller coherent processing intervals (CPIs). For the F-SAR data, each CPI consists has 128 azimuth samples and with a pulse repetition frequency of 2.4 KHz, each CPI has a duration of approximately 53 ms.

The length of the CPI is data and system parameter dependent. Individual CPIs are then transformed into range-Doppler domain via azimuth FFT (fast Fourier transform). The estimated cluster center position (cf. **Section 2**) of the target is then tracked at each CPI.

3.1 Database structure

We have developed a SQLite-based database structure for storing the detection and clustering results and also for doing target tracking. The database has a table where each row of the table represents a detected target at each CPI. The column of each row contains target related parameters. A simplified representation of the database table is shown in **Figure 3**.

Columns (measured motion parameters)

Rows (detected targets)

	Unique ID	CPI (k)	Dopp Freq.(Hz)	Slant Range (m)	Doppler Bin	Range Bin	....	Predicted Flag	Relation	Data Patch
CPI = 0	1	0					....	0	-1	
	2	0					....	0	-1	
	3	0					....	0	-1	
CPI = 1	4	1					....	0	1	
	5	1					....	0	2	
	6	1					....	0	3	
CPI = 2	7	2					....	0	4	
	8	2					....	0	5	
	9	2					....	0	6	
⋮							⋮			

Figure 3 Simplified representation of the database table. Typical values stored for an individual target in the database table are shown.

Figure 3 shows three exemplary targets are detected at CPI = 0. These targets are stored with a unique ID (or unique row number) which increments automatically with subsequent detections in the following CPIs. Other relevant parameters such as the positions of the target, data belonging to the target for ISAR imaging are also stored in the database. The database also has additional columns like predicted flag and relation. Their significance is explained in the later sections.

In the next section we briefly explain the target states and measurements used for tracking targets in range-Doppler domain.

3.2 State and Measurement model

Targets moving with constant velocity on ground have azimuth time dependent Doppler and range histories. This is because the range between the moving radar platform and a specific point of the target on ground changes. The Doppler history of the target mainly varies linearly with time whereas the range is proportional to the time squared. Therefore, the target kinematics in range-

Doppler, i.e., the target's Doppler frequency and range which is assumed to evolve over time can be approximated by constant velocity (CV) and constant acceleration (CA) motion models, respectively.
The received measurements are the target's Doppler frequency and the range positions (cf. **Section 2**). The target states and the measurements discussed in this section are incorporated in the framework of the Kalman filter (KF) [7]. It uses the current measurement, the estimated state and its uncertainty from the previous CPI in order to estimate the true state at the current CPI.
Tracking can even be performed without using any motion model. This is valid only when the targets are detected at every time step and the time steps are relatively small (53 ms in our case). However, without a motion model, target position due to missing detections cannot be predicted and hence large gaps cannot be bridged.

3.3 Maximum manageable gap as motion model performance measure

In real scenarios, it is expected that there will be missing measurements at certain azimuth times. This could be due to the low backscatter received from the moving target or when the target is not illuminated by the antenna beam. In such situations a motion model gives the predicted position (cf. **Section 3.2**). However, inaccurate predictions of the missed measurements may lead to a track loss. Therefore, we have investigated and compared "CV only" and (CV+CA) motion models of the KF to assess their performance in the presence of missed measurements. The (CV+CA) motion model was already briefly discussed in **Section 3.2**. In the "CV only" based motion model along with the Doppler, the range history is also modeled as CV by assuming it as piecewise linear due to the small-time intervals.
For the investigations gaps were artificially introduced in the data (cf. **Figure 4**). The gap time was successively increased to a point after which the target track is lost. The performance achieved from the motion models are compared with the one where no motion model is considered. The results are shown in **Table 1** together with the position accuracies achieved using the methods.

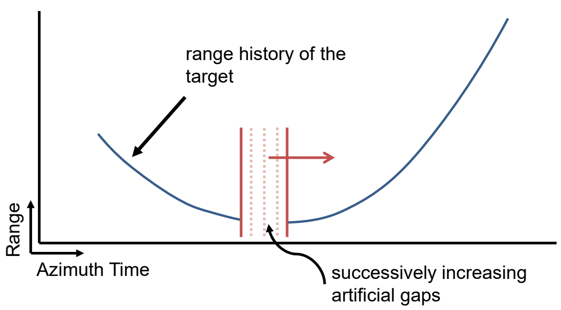

Figure 4 Range history of the moving target shown in range-time domain. Increasing artificially introduced gaps are shown in the figure.

Table 1 shows that in terms of position accuracy all methods perform similar. However, the (CV+CA) motion model is able to maintain the track when the target was invisible for 9.5 s.

Table 1 Analysis of different methods in terms of gap time in seconds after which the target tracks are lost and the position accuracy in Doppler and range. The results are from a real ship signal in real X-band F-SAR airborne radar data.

Methods	Maximum gap time [s]	Position accuracy	
		Doppler RMSE [Hz]	Range RMSE [m]
No motion model	1.6	14.61	0.72
CV	3.4	9.52	1.07
CV+CA	9.5	12.98	0.67

In the next section, we explain the use of relations and unique IDs (cf. **Figure 3**) to form the tracks of arbitrary number of targets.

3.4 Relation generation using database

For tracking targets, it is essential to establish a relation between the detected targets at a given CPI and the already existing detections and tracks from previous CPIs. **Figure 5** shows an example of the concept of relation generation for three targets.

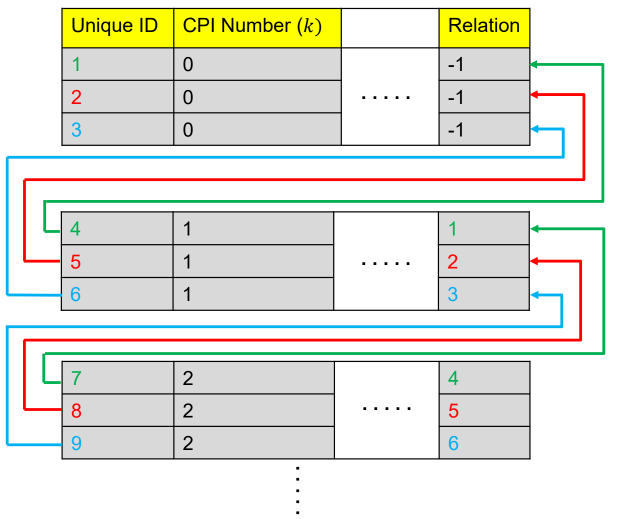

Figure 5 Principle of the relation generation. Arrows of the same colour indicate the link between the unique IDs of same target at each CPI.

As shown in the table, at CPI = 0 there are three detected targets. These targets have unique row numbers. If the same targets are detected in the next CPI, i.e., at CPI = 1, unique row numbers are again generated and the relation column of each target is now updated with the unique row number of the same target from the previous CPI (see relation columns at CPI = 1 and unique ID column in CPI = 0 in **Figure 5**). After the tracking is over, a link between the unique rows belonging to the same target is established (arrows of the same colour in **Figure 5**). A relation of -1 indicates that the target is detected for the

first time and has no relation with any previously existing tracks.
In **Figure 5** it is shown that unique IDs 7-4-1 (green arrow) belong to the same target and likewise for the other two targets.

3.4.1 Data association

In order to create the link between the unique row numbers of the same target at different CPIs, the target detection at current CPI has to be associated with the tracks from the previous CPI. An example is shown in **Figure 6**.

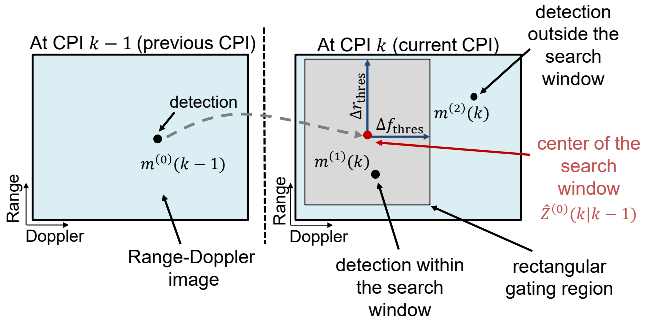

Figure 6 Illustration of the data association concept in range-Doppler domain. Detections in the previous and the current CPI are marked in the figure.

In **Figure 6** at CPI $= k-1$, only one detection (true target cluster center position) is observed which is denoted as $m^{(0)}(k-1)$. At CPI $= k$, two detections are available (see $m^{(1)}(k)$ and $m^{(2)}(k)$). Data association is performed as a two-step procedure. First the position of the target at CPI $= k-1$ is predicted at CPI $= k$ ($\hat{Z}^{(0)}(k|k-1)$ is the KF based prediction of $m^{(0)}(k-1)$). Second a validation region around the predicted position is created. Detection falling with the gate of the track is used for updating the track (cf. **Figure 6** where $m^{(1)}(k)$ lies in the gating region of $\hat{Z}^{(0)}(k|k-1)$.
The rectangular gating criteria shown in **Figure 6** are mathematically expressed as

$$\left|m^{f_{\text{a}}}(k) - \hat{Z}^{f_{\text{a}}}(k|k-1)\right| < \Delta f_{\text{thres}} \quad (1)$$

$$\left|m^{\text{r}}(k) - \hat{Z}^{r}(k|k-1)\right| < \Delta r_{\text{thres}} \quad (2)$$

where $\left|m^{f_{\text{a}}}(k) - \hat{Z}^{f_{\text{a}}}(k|k-1)\right|$ is the offset between the detected and predicted Doppler frequency and $\left|m^{\text{r}}(k) - \hat{Z}^{r}(k|k-1)\right|$ is the offset between the detected and predicted range. The terms Δf_{thres} and Δr_{thres} are the width (along Doppler) and length (along range) of the rectangular region, respectively.
Before determining the extents of the rectangular gate, it is first necessary to investigate how the offsets shown in the left-hand side of (1) and (2) vary so that reasonable values of gate extents can be set. An example of these offsets (also known as innovations) estimated for a real moving ship in real X-band radar data is shown over azimuth time in **Figure 7**.
From **Figure 7**, the maximum observed offsets in Doppler and range are approximately 40 Hz (almost twice the Doppler bin size) and 4 m (almost 14 times the range bin size), respectively.

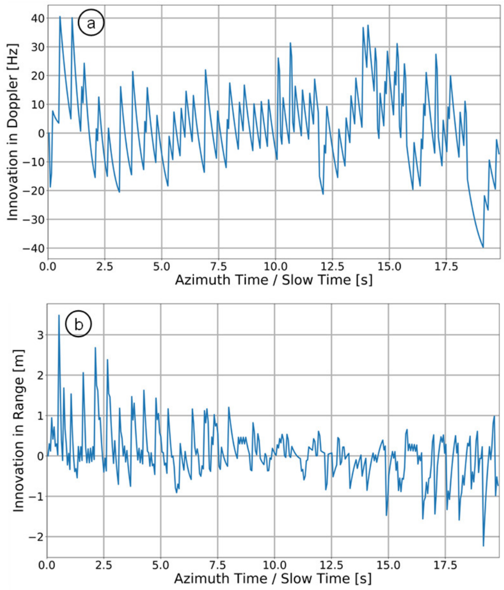

Figure 7 Plots corresponding to the left-hand side of (1) and (2) of a real moving ship, respectively. In KF terminology, these offsets are called innovations or residuals.

The factors that contribute to the instability of the cluster centers are the ship dimensions, their amplitude fluctuations in the data and the Doppler and range bin sizes which for the investigated F-SAR data are approximately 20 Hz and 0.3 m, respectively. The Doppler bin size of 20 Hz corresponds to a resolution of approximately 20 m in cross range.
For the relation generation, the size of the rectangular window must be larger than these maximum observed offsets. A wise choice for the extents of the search window can be set three times the maximum offsets. This will prevent the track loss even if the maximum offsets are a bit larger than what was observed in **Figure 7**.
Note that when there is more than one measurement in the validation region of the track, data association methods based on GNN (global nearest neighbour) or more advanced methods like JPDAF (joint probabilistic data association filter) are recommended [8]. A detailed description of these methods is out of scope of the paper.

4. Track management

Every unassigned detection initiates a tentative track. If this detection belongs to a real target then the target is expected to be detected in several subsequent CPIs. Such a track then becomes a confirmed track. Once the target moves out of the antenna beam, it is no longer detected and therefore should be terminated. To do this, we employ a track management scheme in the tracker which update the confirmed tracks and terminate the finished tracks and false targets. Track management runs periodically. For the F-SAR data, the tracks are checked for e.g., after every 2 s. An example of tracking a single real ship target in X-band HH polarized F-SAR data with and without using track management is shown in **Figure 8.**

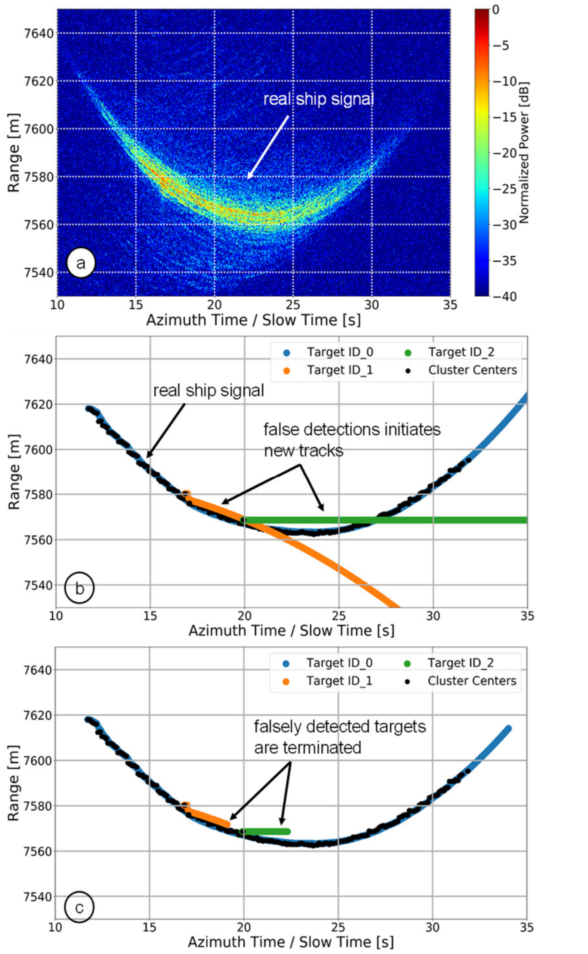

Figure 8 (a) Real single moving ship in real X-band F-SAR radar data. Tracking results without (b) and with (c) track management. Target ID_0 is the trajectory of a real moving ship. For visualization purposes, the tracks are shown in time domain rather in range-Doppler where the detection and tracking were actually carried out.

Track management works in the following way: after every 2 s, individual target tracks are extracted and the predicted flags of each track are checked (cf. **Figure 3** where predicted flag equals zero means, the target is detected or else it is only predicted but not detected). We then calculate a prediction percentage i.e., if the target is predicted more than 70% of the time it is either a false target or has left the antenna beam and therefore is terminated.

As shown in **Figure 8**, Target ID_0 belongs to a real ship target, whereas Target ID_1 and Target ID_2 are the false targets, which are also termed as "ghost targets". With track management it is possible to terminate such target tracks after a short time.

5. Simulation and real experimental results

This section provides some simulation and real experimental results from an F-SAR X-band radar data. In the simulation we considered three moving targets where the effects of missing data and false detections are artificially included. The targets have overlapping range histories. The simulation results are shown in **Figure 9**. For visualization, the trajectories are projected back to time domain. The absolute ground velocity and moving direction of each target are also shown in **Figure 9(b)**.

It is now clear that by using a suitable motion model and track management, the number of targets is reduced from 10 to 3 (plus 2 artificially introduced false detections).

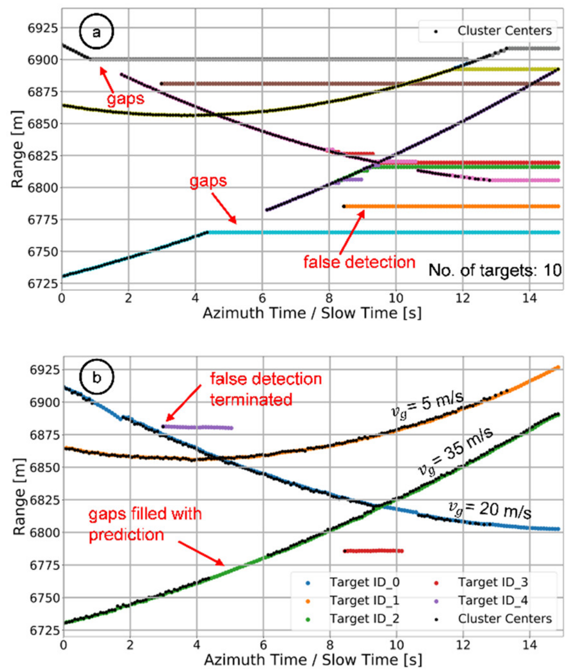

Figure 9 Simulated tracked range histories of three targets (a) without and (b) with considering the motion model and the track management. Artificially introduced gaps and false detections are marked in the figure.

Figure 10 shows the experimental results of real moving ships in real X-band HH polarized airborne radar data. In November 2019, a multi-channel flight campaign using DLR's DBFSAR system was carried out in North Sea near Cuxhaven, Germany. More details related to the radar sensor and the multi-channel data can be found in [4]. The aircraft was flying at an altitude of approximately 2400 m above ground and was also equipped with a dual-channel AIS receiver.

As shown in the **Figure 10 (b)**, there are more than just 2 targets in the ocean data as revealed by the tracking algorithm. In total the tracker tracked 21 targets. Since there is also the track management running in parallel within the tracker, false target tracks like ID_4, ID_6 etc. are terminated after a short time. Using the tracking information, the ship data is also extracted for generating high resolution ISAR image sequences. For demonstration purposes, one of the ISAR image sequences of target ID_15 is shown in **Figure 10 (c)**. The ISAR image is generated by applying the ISAR processor proposed in [9]. The ship name is HAM 316, which is a dredger of dimensions 129 m x 22 m. This ship contains several cranes and booms on the deck, one of them causes a strong multipath reflection which is clearly recognizable in the ISAR image.

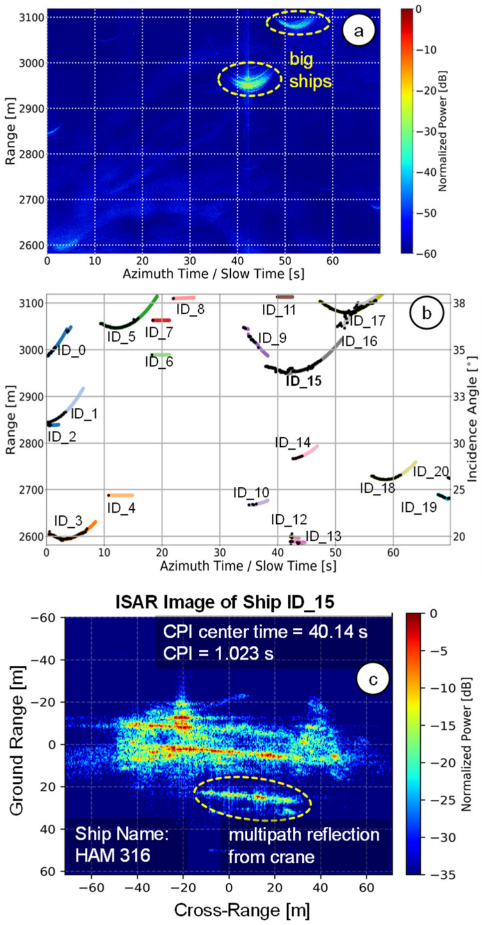

Figure 10 Real RC X-band radar data acquired over the North Sea. Two very bright ships are visible in the figure. (b) Tracking results after applying the proposed algorithm in range-Doppler domain. Ships with individual IDs are shown in the figure. (c) ISAR image of the ship track corresponding to ID_15 from (b).

Since the data shown in **Figure 10(a)** were acquired using multiple receiving channels, the target tracks shown in **Figure 10(b)** can directly be mapped on ground after an additional estimation of the DOA angles of the targets.
A detailed investigation on the ISAR imaging, multichannel data pre-processing, DOA estimation and geocoding techniques are out of scope of the paper.

6. Conclusion

In the paper we have presented some preliminary range-Doppler based ship tracking results using simulated as well as real experimental range-compressed X-band airborne radar data. The algorithm due to the use of mainly azimuth FFTs is expected to have real time capability. The multi-target tracking framework is developed using a SQLite database as core. The database is designed for storing and tracking an arbitrary number of targets, limited only by the available memory and the SQLite limitations. The tracker not only bridges the gaps in the target missing detections but also is able to update the confirmed tracks and terminate the ghost and finished tracks. Although not discussed in detail, when multiple receiving channels are used, the target tracks in range-Doppler as shown in **Figure 10(b)** can be projected on ground after using the estimated DOA angle.

7. References

[1] S. V. Baumgartner, R. Scheiber, F. Bordoni, G. Krieger, and M. Peichl, “HAPS: Potentials, Applications and Requirements for Radar Remote Sensing,” HAPS4ESA - Towards an ESA Stratospheric High Altitude Pseudo-Satellites (HAPS) programme for Earth Observation, Telecommunications and Navigation, 2017.

[2] S. K. Joshi, S. V Baumgartner, A. B. C. Silva, and G. Krieger, “Range-Doppler Based CFAR Ship Detection with Automatic Training Data Selection,” *Remote Sens.*, vol. 11, no. 11, pp. 1270/1-1270/39, 2019.

[3] A. Reigber, R. Horn, A. Nottensteiner, P. Prats, R. Scheiber, K. Bethke and S. V. Baumgartner, “Current status of DLR’s new F-SAR sensor,” in *EUSAR*, 2010, pp. 1078–1081.

[4] A. Reigber, E. Schreiber, K. Trappschuh, S. Pasch, G. Müller, D. Kirchner, D. Geßwein, S. Schewe, A. Nottensteiner, M. Limbach, A. Schreiber, T. Rommel, R. Horn, M. Jäger, R. Scheiber, S. V. Baumgartner, S. K. Joshi, A. B. C. da Silva and A. Moreira, “The high-resolution digital-beamforming airborne SAR system DBFSAR,” *Remote Sens.*, vol. 12, no. 11, 2020.

[5] M. Ester, H.-P. Kriegel, J. Sander, and X. Xu, “A density-based algorithmfor discovering clusters in large spatial databases with noise.,” in *International Conference on Knowledge Discovery and Information Retrieval*, 1996, pp. 226–231.

[6] S. K. Joshi and S. V Baumgartner, “Ship Tracking in High-Resolution Range-Compressed Airborne Radar Data Acquired During Linear and Circular Flight Tracks,” in *RadarConf20*, 2020, pp. 1–6.

[7] R. E. Kalman, “A New Approach to Linear Filtering and Prediction Problems,” *J. Basic Eng.*, vol. 82, no. 1, p. 35, 1960.

[8] Y. Bar-Shalom, F. Daum, and J. Huang, “The probabilistic data association filter,” *IEEE Control Syst. Mag.*, vol. 29, no. 6, pp. 82–100, 2009.

[9] S. V Baumgartner, “Circular and Polarimetric ISAR Imaging of Ships Using Air- borne SAR Sensors,” *EUSAR 2018 12th Eur. Conf. Synth. Aperture Radar, Proc.*, pp. 116–121, 2018.